

## Mangrove biomass estimation in Southwest Thailand using machine learning



Nicholas R.A. Jachowski<sup>a,\*</sup>, Michelle S.Y. Quak<sup>a</sup>, Daniel A. Friess<sup>a</sup>, Decha Duangnamon<sup>b</sup>, Edward L. Webb<sup>c</sup>, Alan D. Ziegler<sup>a,d</sup>

<sup>a</sup> Geography Department, National University of Singapore, AS2-03-01, 1 Arts Link, Kent Ridge, Singapore 117570

<sup>b</sup> Andaman Coastal Research Center for Development, KURDI, Kasetsart University, Ranong 85120, Thailand

<sup>c</sup> Department of Biological Science, National University of Singapore, S-14 Level 6, 14 Science Drive 4, Singapore 117543

<sup>d</sup> Geography Department, National University of Singapore, AS2-04-21, 1 Arts Link, Kent Ridge, Singapore 117570

### A B S T R A C T

**Keywords:**  
Mangroves  
Biomass  
Remote sensing  
Machine learning

Mangroves play a disproportionately large role in carbon sequestration relative to other tropical forest ecosystems. Accurate assessments of mangrove biomass at the site-scale are lacking, especially in mainland Southeast Asia. This study assessed tree biomass and species diversity within a 151 ha mangrove ecosystem on the Andaman Coast of Thailand. High-resolution GeoEye-1 satellite imagery, medium resolution ASTER satellite elevation data, field-based tree measurements, published allometric biomass equations, and a suite of machine learning techniques were used to develop spatial models of mangrove biomass. Field measurements derived a whole-site tree density of 1313 trees ha<sup>-1</sup>, with *Rhizophora* spp. comprising 77.7% of the trees across forty-five 400 m<sup>2</sup> sample plots. A support vector machine regression model was found to be most accurate by cross-validation for predicting biomass at the site level. Model-estimated above-ground biomass was 250 Mg ha<sup>-1</sup>; below-ground root biomass was 95 Mg ha<sup>-1</sup>. Combined above-ground and below-ground biomass for the entire 151-ha stand was 345 (±72.5) Mg ha<sup>-1</sup>, equivalent to 155 (±32.6) Mg C ha<sup>-1</sup>. Model evaluation shows the model had greatest prediction error at high biomass values, indicating a need for allometric equations determined over a larger range of tree sizes.

© 2013 Elsevier Ltd. All rights reserved.

### Introduction

Mangroves are important for their ecological, economic, and societal value (Lacambra, Friess, Spencer, & Moller, 2013; Saenger, 2002). Recent research has focused on the coastal protection value of mangroves, especially following the 2004 Indian Ocean Tsunami (e.g. Barbier, 2006). A recent study in the Indo-Pacific region showed that mangroves play a critical role in carbon sequestration, potentially storing four times as much carbon as other tropical forests, including rainforests (Donato et al., 2011). Since the introduction of Payment for Ecosystem Services (PES) policies, attention has been redirected to quantify the extent to which mangroves sequester carbon, both in standing biomass, as well as the below-ground root biomass and the underlying soil (Alongi,

2011; Kauffman, Heider, Cole, Dwire, & Donato, 2011; World Bank, 2011).

Despite scientific awareness of the large carbon storage potential in mangrove biomass and soils, large areas of mangrove in Southeast Asia have been lost in recent decades to urbanization, aquaculture, timber harvesting and other human activities (Duke et al., 2007; Giri et al., 2008; Valiela, Bowen, & York, 2001). Mangroves along the Andaman coast, for example, have declined an estimated 79% between 1961 and 1989, largely due to anthropogenic activities including aquaculture (Alongi, 2002; Saenger, 2002). In southern Thailand, expansion of intensive shrimp farming is believed to have reduced mangrove extent from 3127 km<sup>2</sup> to 1687 km<sup>2</sup> between 1975 and 1993 (CORIN, 1995).

In recent years, mangrove loss in Thailand has slowed considerably (Barbier & Cox, 2004; EEPSEA, 1998). Some areas, such as the UNESCO Man and Biosphere Reserve in Ranong Province, have been protected from degradation and maintain high tree density (>800 trees ha<sup>-1</sup>) and volume (226 m<sup>3</sup> ha<sup>-1</sup>; Aksornkoe, 1993). However, very little is known about critical mangrove ecosystem characteristics such as biomass and carbon stocks outside of

\* Corresponding author. Tel.: +65 9075 2830.

E-mail addresses: [njachowski@nus.edu.sg](mailto:njachowski@nus.edu.sg), [njachowski@gmail.com](mailto:njachowski@gmail.com) (N.R.A. Jachowski), [michelleqsy@nus.edu.sg](mailto:michelleqsy@nus.edu.sg) (M.S.Y. Quak), [dan.friess@nus.edu.sg](mailto:dan.friess@nus.edu.sg) (D.A. Friess), [psddcd@ku.ac.th](mailto:psddcd@ku.ac.th) (D. Duangnamon), [ted.webb@nus.edu.sg](mailto:ted.webb@nus.edu.sg) (E.L. Webb), [adz@nus.edu.sg](mailto:adz@nus.edu.sg) (A.D. Ziegler).

conservation areas. Assessment of biomass and carbon stocks in these unprotected mangroves can increase their perceived conservation value, in particular through quantification of carbon storage potential, which would make them attractive investments for protection and/or restoration under emerging international mechanisms such as REDD+.

In recognition of the developing financial incentives available for mangrove conservation based on carbon PES schemes, studies are beginning to quantify carbon storage of mangrove ecosystems. Examples include deltaic South Asia (Donato et al., 2011; Mitra, Sengupta, & Banerjee, 2011), Insular SE Asia (Donato et al., 2011), tropical Pacific islands (Donato et al., 2011; Donato, Kauffman, Mackenzie, Ainsworth, & Pflieger, 2012; Kauffman et al., 2011) and karst landscapes in the neotropics (Adame et al., 2013). However, these landscapes differ with mainland SE Asia to varying degrees in terms of geomorphology, sediment input, mangrove species and community structure (Spalding, Blasco, & Field, 1997).

There are many possible approaches to quantifying mangrove forest biomass. The most accurate method is to uproot all the trees to obtain their dry mass. However, this is impractical both due to the cost and effort required and the fact that it would negate the goal of conserving mangrove stands (Ketterings, Coe, Noordwijk, Ambagau, & Palm, 2001). A more reasonable approach is to cut down a few trees and develop a mathematical model relating biomass to measured tree variables, such as diameter at breast height (DBH) and wood density (i.e., allometric equations) (Komiya, Pongpan, & Kato, 2005). The variables can then be measured in a forest to develop biomass estimates. This approach is only practical at the plot scale, great effort is needed to measure all the trees in just 1 ha of mangrove forest. Models based on remotely sensed data are presently the only feasible means of quantifying mangrove forest biomass for forests of areas greater than a few hectares. Such models utilize ground-based data and allometric equations to develop biomass estimates for training forest biomass models based on remotely sensed data such as surface spectral properties and elevation.

There are innumerable statistical models that can be used in developing remote sensing-based models. Traditionally, statistical models can be classified into two categories: data models and machine learning (or algorithmic) models (Breiman, 2001). A main difference between the two is data models assume knowledge of the processes taking place, whereas machine learning models consider the processes complex and unknown (Breiman, 2001). Common data models are linear regression and logistic regression. Common machine learning models are classification and regression trees (CART), support vector machines (SVM) and artificial neural networks (ANN). Where prediction accuracy is the ultimate goal, machine learning models are often superior because they make fewer assumptions about the data and the processes. Data models often assume variables come from a known statistical distribution, such as the normal distribution, which is often an oversimplification. The main argument against machine learning models is that they are often difficult to interpret (Breiman, 2001). However, in modeling scenarios where the priority is developing an accurate model, the best strategy is to employ numerous modeling approaches and select the best resulting model.

Recently, machine learning algorithms have been shown effective for modeling mangrove stand biomass and species distributions using satellite remote sensing data (Heumann, 2011; Huang, Zhang, & Wang, 2009; Wang, Silvan-Cardenas, & Sousa, 2008). However, the majority of mangrove modeling efforts continue to be done using traditional data modeling approaches (e.g. Fatoyinbo, Simard, Washington-Allen, & Shugart, 2008; Simard et al., 2006; Wicaksono, Danoedoro, Hartono, Nehren, & Ribbe, 2011). Machine learning algorithms are often difficult to implement. They also have

not been available as long as traditional data modeling techniques. Recently, a variety of free, open-source software tools have become widely available, including R, WEKA and Python's scikit-learn library (Hall et al., 2009; Pedregosa et al., 2011; R Core Team, 2013). Machine learning is a rapidly growing area of study that should become more common for biomass modeling because of its potential to produce better models than traditional data modeling approaches.

The objective of this study was to develop a mangrove forest biomass model using remotely sensed data and machine learning methods. We also describe an economical assessment approach using widely available remote sensing products and free open-source software for modeling and mapping mangrove biomass.

## Methods

### Study site

This study was conducted within a 151-ha, riverine mangrove situated at the mouth of the Kamphuan River (9°22'N 98°24'E), in Suksamran subdistrict, Ranong Province, along the Andaman Sea in southern Thailand (Fig. 1). The site is located behind a long frontal beach that reduces tidal and wave energy, providing an environment conducive to the establishment of mangrove seedlings (Fig. 1). The mangrove is situated 60 km south of the protected Ranong Biosphere Reserve. Ranong Province has a continuous belt of mangroves along the Andaman Sea coast, comprising almost 80% of all the mangrove forest area in Thailand (Macintosh, Aston, & Havanon, 2002). The coastline of Ranong has undergone less development than other Thai provinces along the Andaman coast (Macintosh, Aston, & Havanon, 2002). However, natural disturbances and anthropogenic activity are causing fragmentation in these mangroves areas (Doydee & Buot, 2010; Macintosh, Aston, & Havanon, 2002). During the 2004 Indian Ocean Tsunami, mangrove trees near the coastline were uprooted by wave surges (Fujioka et al., 2008). Meanwhile, inland areas of mangroves experience bank erosion from boat wakes and deforestation for settlement and aquaculture (Supplementary Fig. S1). Coastal communities in Suksamran subdistrict utilize a range of ecosystem goods and services provided by mangroves – fuelwood, fish, molluscs, crustaceans and other edible and otherwise useful aquatic species are harvested from the mangrove (Macintosh, Ashton, & Tansakul, 2002).

### Field data collection

Trees were measured in 45 separate 20 m × 20 m (400 m<sup>2</sup>) sample plots (total surveyed area = 1.8 ha). Plots were selected using a stratified random sampling method for which strata were initially determined through a qualitative classification of the site into high, medium and low biomass, based on a visual assessment of tree density and size during pre-survey reconnaissance. This stratification was employed to ensure the range of biomass values present in the forest would be sampled. It was necessary to sample plots with both very high and very low biomasses to ensure the models derived from the data would be valid for the entire forest. The plot center points were determined by non-differential GPS to a positional error of <15 m under canopy.

In total, 13, 23, and 9 plots were sampled in low, medium and high density areas of the forest, respectively (Supplementary Fig. S1). Densities corresponded roughly to 45, 55 and 65 trees per 400 m<sup>2</sup> plot. For each tree, we recorded species and diameter at breast height (DBH), which was the diameter at 1.3 m above the ground (or 30 cm above the highest prop root in the case of *Rhizophora* sp.).

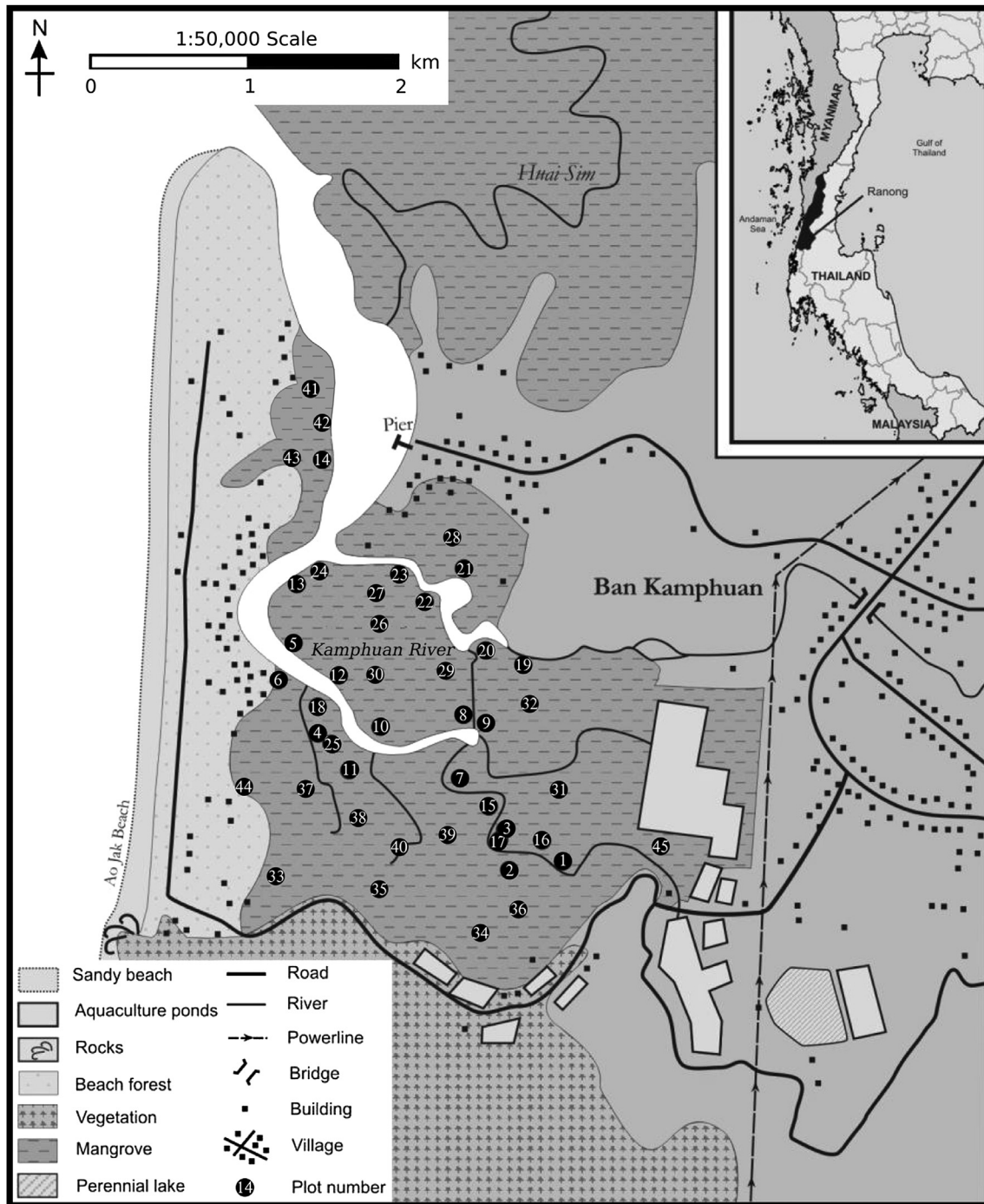


Fig. 1. Map of the study area. Kamphuan River study area (151-ha) and 45 sample plots in Suksamran subdistrict, Ranong province, southern Thailand.

Forest composition, structure, and biomass calculations

Species importance was computed per the importance value index (IVI) (Cintron & Schaeffer Novelli, 1984; Curtis & McIntosh, 1950). Above-ground biomass (AGB) and below-ground biomass (BGB) were computed for each plot using allometric equations developed by Komiyama et al. (2005):

$$AGB = 0.251 * \rho * DBH^{2.46} \tag{1}$$

$$BGB = 0.199 * \rho^{0.90} * DBH^{2.22} \tag{2}$$

where  $\rho$  is species-specific wood density (Table 1). Wood density values were collected in the field for all tree species using a 0.200-inch diameter and 8-inch long handheld tree increment borer and the method described by Komiyama et al. (2005). Three samples were collected for each species. The bark was included for specific gravity wood density measurements with the exception of *Sonneratia ovata* and *Bruguiera gymnorhiza*.

The allometric equations were based on data collected from four sites in southern Thailand (Pang-nga, Trat, Satun and Ranong Provinces) and one in Indonesia (Komiyama et al., 2005). The site in Ranong was located 60 km from our study site. The equations of Komiyama et al. (2005) do not include tree height as a variable, as

**Table 1**  
Mean specific gravity wood density ( $\rho$ ) of 15 mangrove species found at study site.

Species	$\rho$ (Mg m <sup>-3</sup> )
<i>Bruguiera cylindrica</i> (L.) Blume	0.6681 ± 0.057 ( <i>n</i> = 6)
<i>Bruguiera gymnorhiza</i>	0.7273 ± 0.016 ( <i>n</i> = 3) <sup>a</sup>
<i>Bruguiera parviflora</i> (Roxb.) Wight & Griff	0.6256 ± 0.031 ( <i>n</i> = 3)
<i>Ceriops tagal</i> (Perr.) C.B. Rob.	0.6952 ± 0.028 ( <i>n</i> = 6)
<i>Ceriops decandra</i>	0.6952 ± 0.028 <sup>b</sup>
<i>Rhizophora apiculata</i> Blume	0.7417 ± 0.032 ( <i>n</i> = 6)
<i>Rhizophora mucronata</i> Lam.	0.6723 ± 0.054 ( <i>n</i> = 6)
<i>Avicennia alba</i> Blume	0.5220 ± 0.021 ( <i>n</i> = 6)
<i>Avicennia officinalis</i> (L.) Blume	0.5362 ± 0.051 ( <i>n</i> = 6)
<i>Sonneratia alba</i>	0.4110 ± 0.042 ( <i>n</i> = 5)
<i>Sonneratia ovata</i>	0.5502 ± 0.084 ( <i>n</i> = 3) <sup>a</sup>
<i>Xylocarpus granatum</i> Koenig	0.5894 ± 0.021 ( <i>n</i> = 6)
<i>Xylocarpus moluccensis</i> Lam.	0.5495 ± 0.034 ( <i>n</i> = 6)
<i>Lumnitzera littorea</i> (Jack) Voigt	0.5674 ± 0.053 ( <i>n</i> = 6)
<i>Heritiera littoralis</i> (Dryand.) Aiton.	0.6010 ± 0.105 ( <i>n</i> = 6)

Values are ± one standard deviation; *n* is sample number.

<sup>a</sup> Specific gravity wood density was determined without bark.

<sup>b</sup> Assumed to be the same as *Ceriops tagal*.

earlier work has shown that height often does not improve biomass estimations (Ketterings et al., 2001; Soares & Schaeffer-Novelli, 2005; cf. Clough, 1992; Clough & Scott, 1989). To convert above- and below-ground biomass to carbon stocks, the ratio of 0.45 was applied as per Twilley, Chen, and Hargis (1992).

#### Remotely sensed data collection

A geo-corrected GeoEye-1 satellite image (2.0 m spatial resolution with an RMSE of 3.0 m) of the study site was acquired for 14 December 2011. The imagery provides reflectance values in four spectral bandwidths: Band 1 (blue) 450–520 nm; Band 2 (green) 520–600 nm; Band 3 (red) 625–695 nm; and Band 4 (near infrared) 760–900 nm. Radiometric correction was not required because atmospheric effects were consistent across the entire image.

Additionally, medium resolution satellite elevation data (30 m spatial resolution) were acquired from the ASTER GDEM V2 product (NASA LP DAAC, 2012). The ASTER GDEM was chosen because it was available at 30 m resolution for this site, as compared to 90 m resolution for the SRTM DEM. It is also more representative of canopy elevation than the SRTM DEM (Ni, Guo, Sun, & Chi, 2010).

#### Predictor variable selection & preparation

From the remotely sensed data a total of 14 predictor variables were produced and examined (Table 2). In addition to the 4 spectral bands, we also examined 7 combinations of bands: 6 simple ratios (e.g. Band 1/Band 2) and the Normalized Difference Vegetation Index (NDVI). The simple ratio index was first used by Jordan (1969). The Normalized Difference Vegetation Index (NDVI) was calculated as per Rouse, Haas, Schell, and Deering (1973):

$$NDVI = ([\text{Band } 4] - [\text{Band } 3]) / ([\text{Band } 4 + \text{Band } 3]) \quad (3)$$

For all survey plots, spectral reflectance values of bands 1, 2, 3 and 4 were extracted from the image. Due to the large plot sizes (400 m<sup>2</sup>), several GeoEye-1 satellite imagery pixels (4 m<sup>2</sup>) covered each plot. The Band and Ratio variables used the average pixel values in each plot.

The remaining 3 predictor variables were elevation variables. Due to spatial positioning mismatch between the ASTER GDEM pixels and the plot areas there were multiple possible elevation

**Table 2**  
Predictor variables examined in this model-building exercise.

Variable name	Variable definition	Data source
Band 1	Blue, 450–520 nm	GeoEye-1
Band 2	Green, 520–600 nm	GeoEye-1
Band 3	Red, 625–695 nm	GeoEye-1
Band 4	Near infrared, 760–900 nm	GeoEye-1
Ratio 1	Band 1/Band 2	GeoEye-1
Ratio 2	Band 1/Band 3	GeoEye-1
Ratio 3	Band 1/Band 4	GeoEye-1
Ratio 4	Band 2/Band 3	GeoEye-1
Ratio 5	Band 2/Band 4	GeoEye-1
Ratio 6	Band 3/Band 4	GeoEye-1
NDVI	(Band 4 – Band 3)/(Band 4 + Band 3)	GeoEye-1
Minimum elevation	Minimum elevation	ASTER GDEM V2
Maximum elevation	Maximum elevation	ASTER GDEM V2
Average elevation	Average elevation	ASTER GDEM V2

values for each plot. We considered the minimum, maximum and average elevations within the plots.

The selection of predictor variables is always subjective; and there are an infinite possible number of variables that could have been examined. We chose these 14 variables because they are easily accessible to practitioners and simple to compute.

#### Model development

Data preparation, modeling and analysis were carried out using two free and open-source software packages: GRASS GIS and WEKA. GRASS GIS was the geographic information systems software used for data preparation, data extraction at plot locations, and mapping (GRASS Development Team, 2012). WEKA was the modeling software used for machine learning modeling and analysis (Hall et al., 2009). Nineteen WEKA machine learning algorithms were applied to a variety of predictor variable sets (Table 3). Models were ranked according to their correlation coefficients (*r*) with prediction errors based on Leave-One-Out (LOO) cross-validation. In LOO, each sample is excluded in turn and a model developed with all remaining samples is used to predict the excluded sample. This method is useful for identifying outliers and provides nearly unbiased estimations of the prediction error (Efron & Gong, 1983; Schlerf, Atzberger, & Hill, 2005). The 14 predictor

**Table 3**  
WEKA machine learning algorithms used to build above-ground biomass models.

WEKA algorithm	Classifier type	Correlation coefficient
SMOreg	Function	0.81
LeastMedSq	Function	0.78
GaussianProcesses	Function	0.77
PaceRegression	Function	0.74
LinearRegression	Function	0.74
MSP	Trees	0.74
M5Rules	Rules	0.73
SimpleLinearRegression	Function	0.72
IsotonicRegression	Function	0.66
LWL	Lazy	0.61
DecisionStump	Trees	0.60
MultilayerPerceptron	Function	0.59
lbc	Lazy	0.56
RBFNetwork	Function	0.54
Kstar	Lazy	0.53
REPTree	Trees	0.42
ConjunctiveRule	Rules	0.40
DecisionTable	Rules	0.30

The algorithms are ranked by correlation coefficients determined using a leave-one-out analysis of models constructed using the optimal predictor variable set: Band 2, Band 4, Ratio 1, Minimum & Maximum elevations (see Table 6). Algorithm descriptions can be found at <http://www.cs.waikato.ac.nz/ml/weka/> (Hall et al., 2009).

variables were examined in various combinations (Table 2). As it would have been inefficient to test all possible combinations of predictor variables across all modeling techniques (a total of 311,277 combinations), a heuristic approach was taken to determine possible combinations that would yield better models. The overall goal of the model development process was to determine the most accurate model for spatial biomass prediction.

## Results

### Field survey results

A total of 2364 trees were recorded in the 45 survey plots, representing a combined area of 1.8-ha. Fifteen species were found at the site: *Rhizophora apiculata*, *Rhizophora mucronata*, *Bruguiera cylindrica*, *Bruguiera parviflora*, *B. gymnorhiza*, *Ceriops tagal*, *Ceriops decandra*, *Heritiera littoralis*, *Lumnitzera littorea*, *Sonneratia alba*, *S. ovata*, *Xylocarpus granatum*, *Xylocarpus moluccensis*, *Avicennia alba* and *Avicennia officinalis*. Two mangrove associates were recorded: *Calophyllum inophyllum*

( $n = 2$ ) and *Intsia bijuga* ( $n = 1$ ), but not included in species importance or biomass calculations.

Tree counts ranged from 0 to 106 trees per plot (Table 4). The 0 tree plot contained mangrove trees of DBH < 4.5 cm, which is below the threshold for biomass determination using the allometric equations. Density of the 1.8-ha sample area was 1313 trees ha<sup>-1</sup> (Table 4). High total tree count and relative density were found for *R. apiculata* (1461 trees; 61.8%) and *R. mucronata* (375 trees; 15.9%; Table 5). Importance value indices for the two dominant *Rhizophora* species were 151 and 51, respectively (Table 5). *A. alba* had the third highest dominance (1.973 m<sup>2</sup> ha<sup>-1</sup>), but only the fourth highest importance value (IVI = 18), lower than that of *X. granatum* (IVI = 25). This anomaly occurs because relatively few *A. alba* trees were present, but they were large in size compared to the other dominant species.

Total above-ground biomass in each 400 m<sup>2</sup> plot ranged from 0 to 18,000 kg (median = 9393 kg). Estimated below-ground biomass in each plot ranged from 0 to 6080 kg (median = 3626 kg). The overall ratio of BGB to AGB was 0.38. This ratio is calculated using

**Table 4**  
Summary of mangrove tree data per plot ( $n = 45$ ).

Plot	Trees per 400 m <sup>2</sup>	Trees per ha	Basal area (m <sup>2</sup> )	Mean DBH	AGB kg/400 m <sup>2</sup>	BGB kg/400 m <sup>2</sup>	AGB Mg ha <sup>-1</sup>	BGB Mg ha <sup>-1</sup>
1	43	1075	1.385	18.871	13,817.337	5142.297	345.433	128.557
2	42	1050	1.043	15.807	10,335.440	3883.472	258.386	97.087
3	53	1325	1.095	14.916	9921.330	3856.719	248.033	96.418
4	52	1300	0.705	11.981	5776.360	2341.560	144.409	58.539
5	64	1600	1.610	12.966	17,991.740	5647.671	449.794	141.192
6	29	725	0.487	13.974	3988.444	1629.497	99.711	40.737
7	48	1200	1.193	16.197	11,408.271	4322.438	285.207	108.061
8	60	1500	1.435	15.187	14,325.243	5352.087	358.131	133.802
9	53	1325	1.110	15.027	10,132.869	3938.587	253.322	98.465
10	39	975	1.438	17.092	15,794.104	5121.420	394.853	128.036
11	51	1275	1.063	14.549	9439.333	3619.454	235.983	90.486
12	74	1850	1.000	11.953	7885.815	3214.068	197.145	80.352
13	42	1050	0.913	14.869	7589.502	2893.871	189.738	72.347
14	15	375	0.679	21.985	5797.062	2062.049	144.927	51.551
15	39	975	1.027	17.061	9895.858	3773.957	247.396	94.349
16	59	1475	1.143	14.415	10,230.254	3979.934	255.756	99.498
17	48	1200	1.037	15.277	9347.317	3633.146	233.683	90.829
18	72	1800	1.104	12.899	8516.277	3446.974	212.907	86.174
19	37	925	0.893	15.141	8188.038	3040.095	204.701	76.002
20	29	725	0.800	17.011	7889.736	2957.445	197.243	73.936
21	72	1800	1.082	12.264	8766.425	3446.435	219.161	86.161
22	62	1550	0.996	13.020	8779.973	3501.067	219.499	87.527
23	83	2075	0.739	9.860	5413.933	2325.818	135.348	58.145
24	31	775	1.025	17.566	8911.346	3179.487	222.784	79.487
25	50	1250	0.792	12.205	6489.086	2524.649	162.227	63.116
26	59	1475	0.995	13.561	8241.872	3299.101	206.047	82.478
27	106	2650	1.548	12.525	12,646.697	5147.821	316.167	128.696
28	78	1950	1.160	11.887	10,278.548	4062.997	256.964	101.575
29	51	1275	0.982	14.502	8441.013	3338.528	211.025	83.463
30	57	1425	1.474	16.471	13,577.793	5162.475	339.445	129.062
31	58	1450	1.214	14.660	11,400.768	4396.304	285.019	109.908
32	50	1250	1.344	17.199	12,271.223	4661.985	306.781	116.550
33	48	1200	1.342	17.814	12,356.818	4715.881	308.920	117.897
34	57	1425	1.220	15.550	10,988.155	4316.823	274.704	107.921
35	55	1375	1.175	15.289	10,829.073	4215.957	270.727	105.399
36	54	1350	1.641	18.236	16,129.336	6078.785	403.233	151.970
37	60	1500	0.851	12.182	7169.080	2903.372	179.227	72.584
38	72	1800	1.245	13.801	10,823.914	4321.418	270.598	108.035
39	57	1425	0.920	12.211	8488.238	3267.708	212.206	81.693
40	60	1500	1.111	14.285	9846.540	3899.712	246.163	97.493
41	20	500	0.055	5.392	188.231	93.603	4.706	2.340
42	0	0	0.000	0.000	0.000	0.000	0.000	0.000
43	87	2175	0.185	4.628	674.206	336.815	16.855	8.420
44	74	1850	0.101	3.351	497.617	240.983	12.440	6.025
45	14	350	0.620	20.583	5753.584	1988.690	143.840	49.717
<b>Average</b>	<b>53</b>	<b>1313</b>	<b>0.999</b>	<b>13.916</b>	<b>9049.640</b>	<b>3450.737</b>	<b>226.241</b>	<b>86.268</b>

DBH is diameter at breast height; AGB is above-ground biomass; BGB is below-ground biomass. The ratio of BGB to AGB is 0.38.

**Table 5**  
Importance value index (IVI) and other indices for each species present in this study.

Species	Count	Density (no. of trees/plot)	RD (%)	Frequency	RF (%)	Basal area (m <sup>2</sup> )	Dominance (m <sup>2</sup> ha <sup>-1</sup> )	RD <sub>o</sub> (%)	IVI
<i>R. apiculata</i>	1461	32.47	61.80	0.93	22.58	30.100	16.722	66.922	151.30
<i>R. mucronata</i>	375	8.33	15.86	0.73	17.74	7.693	4.274	17.105	50.71
<i>X. granatum</i>	113	2.51	4.78	0.64	15.59	1.964	1.091	4.366	24.74
<i>B. cylindrica</i>	81	1.80	3.43	0.31	7.53	0.368	0.205	0.819	11.77
<i>S. alba</i>	71	1.58	3.00	0.04	1.08	0.138	0.077	0.308	4.39
<i>A. alba</i>	63	1.40	2.66	0.29	6.99	3.552	1.973	7.898	17.55
<i>L. littorea</i>	54	1.20	2.28	0.02	0.54	0.037	0.021	0.083	2.90
<i>C. tagal</i>	50	1.11	2.12	0.33	8.06	0.199	0.110	0.442	10.62
<i>A. officinalis</i>	30	0.67	1.27	0.20	4.84	0.422	0.235	0.939	7.05
<i>B. parviflora</i>	24	0.53	1.02	0.22	5.38	0.318	0.177	0.707	7.10
<i>X. moluccensis</i>	23	0.51	0.97	0.29	6.99	0.095	0.053	0.212	8.17
<i>S. ovata</i>	12	0.27	0.51	0.02	0.54	0.023	0.013	0.052	1.10
<i>H. littoralis</i>	5	0.11	0.21	0.04	1.08	0.052	0.029	0.117	1.40
<i>C. decandra</i>	1	0.02	0.04	0.02	0.54	0.001	0.001	0.003	0.58
<i>B. gymnorhiza</i>	1	0.02	0.04	0.02	0.54	0.013	0.007	0.028	0.61
<b>Total</b>	<b>2364</b>	<b>52.53</b>	<b>100.00</b>	<b>4.13</b>	<b>100.00</b>	<b>44.98</b>	<b>24.987</b>	<b>100.00</b>	<b>300.00</b>

RD is relative density; RF is relative frequency; RDo is relative dominance; frequency refers to the percentage of the 45 plots containing the species. The important value is calculated as:  $IVI = RD + RF + RDo$ , where relative density (RD), relative frequency (RF), and relative dominance (RDo) can add up to a maximum value of 300 (per [Cintron & Schaeffer Novelli, 1984](#); [Curtis & McIntosh, 1950](#)).

the average BGB (Mg ha<sup>-1</sup>) and AGB (Mg ha<sup>-1</sup>) of all the recorded plots; and it is in general agreement with the root:shoot ratios reviewed by [Yuen, Ziegler, Webb, and Ryan \(2013\)](#) and [Ziegler et al. \(2012\)](#).

#### Model selection

Examination of the histograms of the 14 predictor variables clearly shows which variables had more variation, and therefore might make better predictors ([Fig. 2](#)). Half of the variables could be discarded using this observation (Ratio 3, Ratio 4, Ratio 5, Ratio 6, Band 1, Band 3, NDVI). The correlation coefficients ( $r$ ) of various combinations of the 14 predictor variables illustrates that discarding these seven variables did not affect model accuracy negatively ([Table 6](#)). Of all the combinations examined, the set of variables found to produce the optimal models were Band 2, Band 4, Ratio 1, Minimum elevation and Maximum elevation ([Table 6](#)). The model with the highest correlation coefficient ( $r$ ) was a support vector machine regression model developed using the SMOreg algorithm ([Table 3](#); [Shevade, Keerthi, Bhattacharyya, & Murthy, 1999](#); [Smola & Schoelkopf, 2004](#)).

#### Model results

The best AGB model came from a support vector machine regression with the following equation:

$$AGB = 0.16 * [Elevation] + 0.27 * [Band 1] / [Band 2] - 0.11 * [Band 2] + 0.41 * [Band 4] - 0.03 \quad (4)$$

where all variables are normalized to the range 0–1; Band 1 is the blue spectral band (450–520 nm); Band 2 is the green spectral band (520–600 nm); and Band 4 is the near infrared spectral band (760–900 nm). This model had a correlation coefficient of 0.81. The model originally contained terms for minimum and maximum elevations, however because we applied this model at 2-m resolution rather than the 20-m resolution of the sample plots, there were no longer overlapping elevation pixels, therefore each 2-m pixel only contained a single elevation value. This necessitated the collapse of the minimum and maximum elevation variables into one elevation term in the final model (Equation (4)).

To evaluate model performance, observed and predicted biomass values were plotted and the two variables were regressed

as per [Pineiro, Perelman, Guerschman, and Paruelo \(2008; Fig. 3\)](#). The slope of the regression was 0.15 units greater than the slope of the 1:1 line and was highly significant at  $p < 0.0001$ , which indicates the model over-estimates biomass at low observed values and under-estimates at high values. The intercept of the regression was not significantly different from zero. As the null hypothesis for the slope was rejected, but that for the intercept was accepted, the model is said to be unbiased ([Pineiro et al., 2008](#)). Computing the Theil's coefficients shows that the majority of the variance in the observed values which are not explained by the model is due to unexplained variance ( $U_{error} = 93\%$ ; [Paruelo, Jobbagy, Sala, Lauenroth, & Burk, 1998](#)). The model had a coefficient of determination ( $r^2$ ) of 0.66 and was highly significant at  $p < 0.0001$ . The Root-Mean-Square Deviation (RMSD) estimates the mean deviation of the model predictions from the observed values to be 53.4 Mg ha<sup>-1</sup>. As the model has been shown to be unbiased, the RMSD is the standard error of the model.

The above-ground biomass for the 151-ha Kamphuan mangrove, as computed by Equation (4), was  $250 \pm 53.4$  Mg ha<sup>-1</sup> with the highest carbon stocks located in the mangrove interior and the landward edge ([Fig. 4](#)). Using the 0.38 ratio of below-ground to above-ground biomass yielded an estimated below-ground biomass of 95 Mg ha<sup>-1</sup> (see legend in [Table 4](#)). Combined AGB and BGB at the site was  $345 \pm 72.5$  Mg ha<sup>-1</sup>. Using the 0.45 conversion factor between biomass and carbon stock ([Twilley et al., 1992](#)), the estimated above- and below-ground carbon biomass was 113 and 42.8 Mg C ha<sup>-1</sup>, respectively.

## Discussion

### Mangrove community composition and biomass

Fifteen mangrove tree species were found at our study site along the Kamphuan River. This represents higher species diversity than has been found previously in Ranong and Trang Provinces of Southern Thailand ([Table 7](#)). Previously, the highest recorded species diversity was found at the Mangrove Forest Research Center in Ranong by [Kongsangcha et al. \(1993\)](#) and [Macintosh, Aston, and Havanon \(2002\)](#), where twelve species were recorded. Eleven species were reported for Rachakrud subdistrict and as few as six species were recorded elsewhere in Ranong ([Doydee & Buot, 2010](#); [Tamai & Iampa, 1988](#); [Table 7](#)). These differences in species diversity among nearby study sites could be an artifact of sampling design

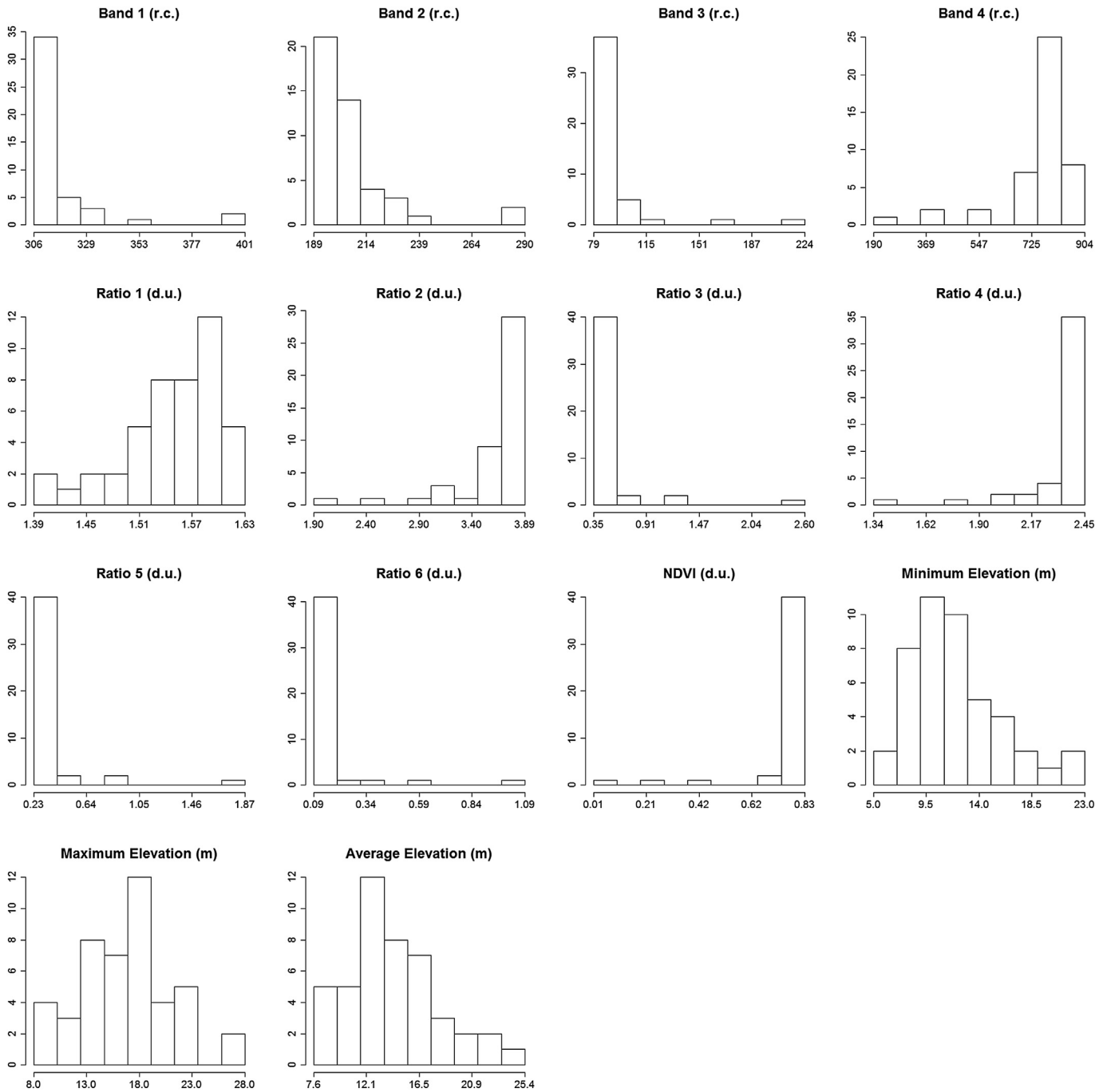


**Fig. 2.** Histograms of predictor variables. Histograms of the 14 predictor variables examined in this modeling exercise. Elevation values are in meters (m), band values are in reflectance counts (r.c.) and ratio and NDVI values are dimensionless units (d.u.). Examination of the histograms shows clearly which variables have more variation, and therefore might make better predictors. Half of the variables could be discarded using this observation (Ratio 3, Ratio 4, Ratio 5, Ratio 6, Band 1, Band 3, NDVI). The data in Table 6 illustrate that discarding these seven variables did not negatively affect model results. Of all the combinations examined, the set of variables found to produce the optimal models were Band 2, Band 4, Ratio 1, Minimum elevation and Maximum elevation.

which may miss rare species, particularly given the dominance of *Rhizophora* species found at our site: *R. apiculata* was present in 42 out of 45 plots, and it was dominant in 33; *R. mucronata* was present in 33 plots, and dominant in 6.

The AGB at our Kamphuan River site is on the high end of values reported for other Thai mangroves. In a comparison of eight studies, AGB in Thai mangrove sites ranged from 62 to 299 Mg ha<sup>-1</sup>, with this study coming in at the second highest with 250 Mg ha<sup>-1</sup> (Table 8). Not surprisingly, the AGB values

follow a gradient of disturbance with sites exhibiting more human disturbance (e.g. secondary forests) having less AGB. However, human disturbance doesn't necessarily lead to decreased AGB – the site with the highest recorded mangrove AGB in Southeast Asia was in a mature, *Rhizophora*-dominated stand in Matang, Malaysia, where the mean AGB was 409 Mg ha<sup>-1</sup> (Putz & Chan, 1986). Much of the Matang mangrove is intensively farmed on a cutting rotation for charcoal production, so it is not representative of natural mangrove, but rather a highly disturbed and

**Table 6**  
Predictor variable pruning showing the correlation coefficients of the SMOreg model developed using the selected predictor variables.

Correlation coefficient	Band 1	Band 2	Band 3	Band 4	Ratio 1	Ratio 2	Ratio 3	Ratio 4	Ratio 5	Ratio 6	NDVI	Minimum elevation	Maximum elevation	Average elevation
0.81 <sup>a</sup>		*		*	*							*	*	*
0.81		*		*	*							*	*	*
0.80	*	*	*	*	*	*		*				*	*	*
0.80		*	*	*	*	*		*				*	*	*
0.80		*	*	*	*	*		*				*	*	*
0.80		*	*	*	*	*		*				*	*	*
0.79		*	*	*	*	*	*	*	*	*	*	*	*	*
0.77	*	*	*	*	*	*	*	*	*	*	*	*	*	*
0.77	*	*	*	*	*	*	*	*	*	*	*	*	*	*
0.77	*	*	*	*	*	*	*	*	*	*	*	*	*	*
0.77	*	*	*	*	*	*	*	*	*	*	*	*	*	*
0.66					*							*	*	*
0.36												*	*	*

Shaded and starred boxes indicate which predictor variables were used in each model – a white box indicates the variable was not used.

<sup>a</sup> The most accurate model, generated using Band 2, Band 4, Ratio 1, Minimum elevation and Maximum elevation. Notably, the correlation coefficients drop off considerably when fewer variables are used.

highly managed mangrove. The initial planting spacing of 1.2–1.8 m is considerably more dense than found naturally at our Kamphuan River site (Alongi, 2011; Muda & Mustafa, 2003).

As forest structure and composition evolve over time due to ecological responses to physical and chemical changes in the ecosystem, species density and carbon storage also change (Alongi, 2011). With the exception of the largest individuals, most of the trees in the *Rhizophora*-dominated Kamphuan River mangrove stand are about 22–27 years old (Fujioka et al., 2008). Thus, canopy production has likely reached its peak, which generally occurs after 25–30 years in *R. apiculata* plantations in Southeast Asia (Alongi, 2011). Production should continue at this level for more than another 80 years (Alongi, 2011). With changes expected in forest

dynamics over the decades, subsequent studies could focus on how carbon storage changes in natural versus disturbed stands.

*An appraisal of techniques to estimate above-ground biomass and carbon storage in mangroves*

Remote sensing-based models are the most feasible option to develop stand biomass estimates in mangrove forests with areas greater than a few hectares; however, they can only be as good as the input data and the models used to derive those data. This study produced a remote sensing model for biomass based on plot data derived from allometric equations using tree measurements collected in the field. The allometric equations were derived from a small number of trees ( $n = 104$ ), and were only based on trees with DBHs of less than 48.9 cm (Komiyama et al., 2005). Therefore, the accuracy of the equation is known only for relatively small trees. This may explain why evaluation of the remote sensing model showed the model over-estimated biomass at low observed values, under-estimated at high values, and showed greatest error at high biomass values. Plots of high biomass contain the largest trees,

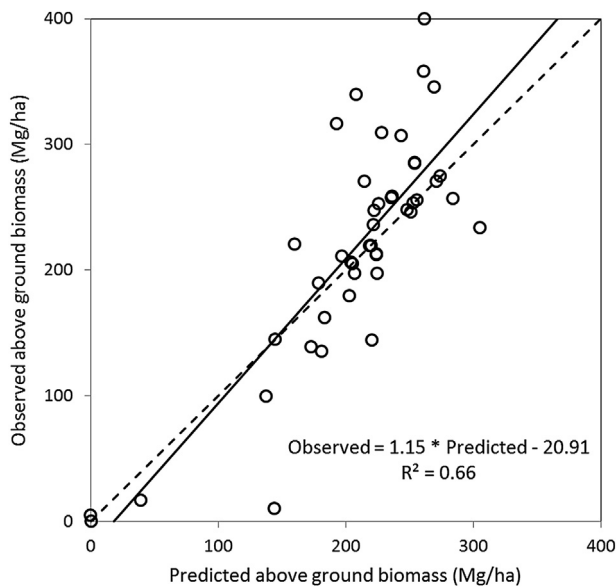


**Fig. 3.** Predicted versus observed biomass. Predicted versus observed biomass in each of forty-five sample plots. Predicted biomass was computed using a support vector machine regression and observed biomass was computed using an allometric equation involving field-measured tree DBH and wood density data. The dashed line indicates the 1:1 line of perfect agreement. The solid line indicates the regression of observed versus predicted biomass, and the equation shows the slope and intercept values of this regression. The model has a coefficient of determination of 0.66 and is highly significant at  $p < 0.0001$ . The regression line indicates the model over-estimates biomass at low observed values and under-estimates at high values.

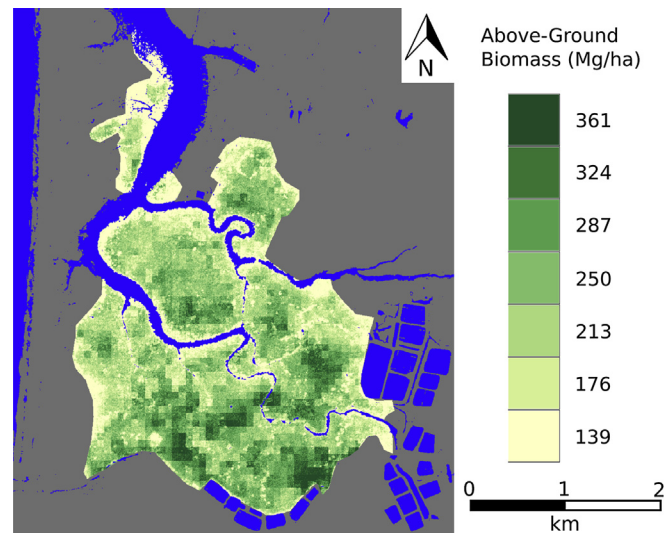


**Fig. 4.** Map of mangrove biomass. Spatial distribution of above-ground biomass per hectare in the 151-ha Kamphuan mangrove. Values are presented in intervals of  $\pm 0.5$  standard deviation from the mean above-ground biomass of  $250 \text{ Mg ha}^{-1}$ . One standard deviation is equal to  $74 \text{ Mg ha}^{-1}$ .

**Table 7**  
Comparison of species presence and dominance in other study sites in Ranong, Trang, Phuket and Phangnga Provinces in Thailand.

Species name	Family	A	B	C	C	D	D	E	E	F	F	G	G	H	H	I	J	K	L	M	N	O	P	Q
<i>Aegiceras corniculatum</i>	Myrsinaceae	p	p					p			p					p			p				p	
<i>Avicennia alba</i>	Avicenniaceae	p							p	p	p					p			p	p				
<i>Avicennia marina</i>	Avicenniaceae	p								102	p	p	p			p			p		p			
<i>Avicennia officinalis</i>	Avicenniaceae	p	p	p	p	p	p	p	p	88	p					p							p	p
<i>Bruguiera cylindrica</i>	Rhizophoraceae	p	p					p	p	p	p			p	p	p	p	*				p	p	91
<i>Bruguiera gymnorrhiza</i>	Rhizophoraceae	p								p							p	p	*					
<i>Bruguiera parviflora</i>	Rhizophoraceae	p	p	103	p	p	p	p	p	p				p	77	p	p		p		p			
<i>Ceriops decandra</i>	Rhizophoraceae	p	p			p	p	p	p			99	105			p	p	p	p	p	p	p		
<i>Ceriops tagal</i>	Rhizophoraceae	p	p	p	p	p		p	p					p	p	p			p			p	p	p
<i>Derris indica</i>	Fabaceae	p	p																				p	
<i>Excoecaria agallocha</i>	Euphorbiaceae	p									p	p	p											
<i>Heritiera littoralis</i>	Sterculiaceae	p										p					p	p					p	
<i>Lumnitzera littorea</i>	Combretaceae	p										p	p											
<i>Lumnitzera racemosa</i>	Combretaceae	p										p												
<i>Rhizophora apiculata</i>	Rhizophoraceae	151	131	p	p	120	177	190	112	p	p	p	p	p	107	p	*	*	*	p	178	130	44	p
<i>Rhizophora mucronata</i>	Rhizophoraceae	p	p	p	120	p	p		p	p				p	p	p	p	p	p	p	p			p
<i>Scyphiphora hydrophyllacea</i>	Rubiaceae	p											p											
<i>Sonneratia alba</i>	Sonneratiaceae	p	p							p	p			p	p	p		p	*					p
<i>Sonneratia ovata</i>	Sonneratiaceae	p																						
<i>Xylocarpus granatum</i>	Meliaceae	p	p	p			p	p		p	p	p	p	p	p	p							p	p
<i>Xylocarpus moluccensis</i>	Meliaceae	p	p	p		p			p	p							p					p	p	
Total no. of species		15	12	7	5	7	7	8	9	11	11	9	8	7	6	13	6	5	8	6	5	5	5	10

'p' indicates species was present in the case study (letters A to P), numbers are reported IVI values of dominant species; 'p' indicates presence of species reported by local guides but was not recorded in our plots; '\*' indicates a dominant species for which no IVI value was reported.

- (A) Ranong Province, Kamphuan village (this study).
- (B) Ranong Province, Mangrove Forest Research Center (Kongsangcha et al., 1993; <http://www.nacsj.or.jp/pn/houkoku/h01-08/h03-no19.html>).
- (C) Ranong, Suksamran District, Talaynog Village (Doydee & Buot, 2010).
- (D) Ranong, Suksamran District, Hadsaykaow Village (Doydee & Buot, 2010).
- (E) Ranong, Ngaw Village (Doydee & Buot, 2010).
- (F) Ranong, Rachakrud Village (Doydee & Buot, 2010).
- (G) Ranong, Kapoe District, Bangben Village (Doydee & Buot, 2010).
- (H) Ranong, Kapoe District, Banghin Village (Doydee & Buot, 2010).
- (I) Ranong, Mangrove Forest Research Center, northern Klong Ngao Village (Macintosh, Aston, & Havanon, 2002).
- (J) Ranong, Kapoe District, Klong Naka Village (Tamai & Iampa, 1988).
- (K) Ranong, Hatsuikhaio Village (Komiya, Ogino, Aksornkoae, & Sabhasri, 1987) – only species zones mentioned.
- (L) Ranong, Hatsuikhaio District, Klong Ngao Village (Permanent transect; Tamai, Nakasuga, Tabuchi, & Ogino, 1986).
- (M) Ranong, Hatsuikhaio District, Klong Ngao Village (Subplot of transect, Sonneratia zone; Tamai et al., 1986).
- (N) Trang, Laem Makham (Community forest; Sudtongkong & Webb, 2008) – only top 5 most important.
- (O) Trang, To Ban (State forest; Sudtongkong & Webb, 2008) – only top 5 most important.
- (P) Phuket, Ko Yao Yai (Chansang, 1984).
- (Q) Phangnga, Mangrove Habitat Study Area (Phongsuksawat, 2002).

whose biomasses are likely under-estimated using Equation (1). Despite these limitations, the remote sensing biomass model developed in this study was able to derive an AGB estimate for the Kamphuan River mangrove with a standard error of ±21% based on Leave-One-Out cross-validation.

Improving these larger-than-plot scale biomass models will require improving the raw data, particularly those regarding the allometric equations upon which plot biomass data are derived. As noted, larger trees need to be included in the derivation of allometric equations if the biomasses of large trees are to be modeled with any certainty. However, the destructive sampling of large trees is undesirable to most researchers. An alternative is to develop non-destructive methods of measuring tree biomasses. A promising, size-independent method is three dimensional (3D) modeling. New technology allows anyone with a digital camera and internet-access the ability to develop 3D models (e.g. Autodesk, 2013; My3DScanner, n.d.) that could be used to compute tree volumes, which, together with wood density, remote sensing derived tree height and other non-destructive measurements could be used to estimate tree biomasses (e.g. Fatoyinbo et al., 2008; Simard et al., 2006; Simard, Fatoyinbo, & Pinto, 2009).

While the model presented here was shown to be the optimal model at this site and given this particular set of training data, practitioners should be wary of applying this model to other sites, particularly sites with dissimilar species composition and at sites

located outside Ranong Province, unless they have determined model accuracy by collecting ground data using the methods described in this paper.

Additionally, while the method of model development illustrated here is feasible for areas on the scale of several hundred hectares, it becomes less feasible at larger scales due to the prohibitive cost of acquiring high-resolution imagery. At those larger scales, methods involving MODIS and Landsat imagery have been shown effective for mapping carbon stocks and landcover change (e.g. Chen, Li, Liu, & Ai, 2013; Klein, Gessner, & Kuenzer, 2012).

### Conclusions and management implications

The Kamphuan River mangrove stand was dominated by two *Rhizophora* species (*R. apiculata* and *R. mucronata*) that comprised about 77.7% of the total tree count. The estimated tree carbon for the 151 ha site was  $155 \pm 32.6 \text{ Mg C ha}^{-1}$  (above-ground carbon biomass =  $113 \text{ Mg C ha}^{-1}$ , below-ground carbon biomass =  $42 \text{ Mg C ha}^{-1}$ ). These estimates were developed using high-resolution GeoEye-1 satellite imagery, medium resolution ASTER satellite elevation data, field-based biomass data, and a support vector machine regression model. The model shows greatest prediction error in the upper ranges of observed biomass suggesting a need for allometric equations calibrated over a larger

**Table 8**  
Comparison of tree density, above-ground biomass (AGB) and below-ground biomass (BGB) at several sites in Thailand, and one in Malaysia.

Province (site)	AGB (Mg ha <sup>-1</sup> )	Forest type	Dominant species	Reference
Perak, Malaysia (Matang)	409	Plantation	<i>R. apiculata</i>	Putz and Chan (1986)
Ranong (Ranong Biosphere Reserve)	281–299	Primary	Mixed spp.	Komiyama et al. (1987) and Tamai et al. (1986)
Ranong (Kamphuan River)	250	Primary	<i>R. apiculata</i>	This study
Chumphon (Sawi Bay)	216	Plantation	<i>Rhizophora</i> spp.	Alongi and Dixon (2000) in Komiyama et al. (2008)
Phuket	159	Secondary	<i>R. apiculata</i>	Christensen (1978)
Trat	142	Secondary	Mixed spp.	Poungparn (2003) in Komiyama et al. (2008)
Pang-nga	108	Secondary	Mixed spp.	Phongsuksawat (2002)
Satun	92	Secondary	<i>C. tagal</i>	Komiyama et al. (2000) in Komiyama et al. (2008)
Pang-nga	62	Secondary	Mixed spp.	Poungparn (2003) in Komiyama et al. (2008)

range of tree sizes. The estimated total biomass of  $345 \pm 72.5$  Mg ha<sup>-1</sup>, high density (1313 trees ha<sup>-1</sup>), and presence of 15 mangrove species indicates this mangrove forest is in good health despite being located in an area where encroachment for aquaculture and timber extraction are of increasing concern.

These observations provide valuable information for mangrove change monitoring and management in Southern Thailand where coastal development has, and likely will continue to result in substantial changes to the natural environment. Since the 2004 Indian Ocean Tsunami, conservation groups have begun mangrove revegetation projects in the area. These and other mangrove conservation efforts will benefit from knowledge gained in studies such as ours. In the meantime, mangrove conversion for shrimp aquaculture, timber and urban development are still immediate threats, which have greatly affected surrounding shorelines in Thailand. Furthermore, accelerated sea level rise may prove a key tipping point to long-term mangrove survival (Friess et al., 2012), particularly in locations such as the Kamphuan River where mangrove migration to higher elevations is constricted by landward human structures. Accurate information on standing carbon stocks provides a financial justification for the better protection, management and rehabilitation of these critical coastal ecosystems.

## Acknowledgment

MSYQ, NRAJ and ADZ were supported by the Singapore Delft Water Alliance (SDWA) JBE (Joint Singapore Marine Program) grant #303-001-020-414. DAF and ELW acknowledge SDWA, NUS (264-001-024-272/414). The ASTER GDEM V2 data were obtained through the online Data Pool at the NASA Land Processes Distributed Active Archive Center (LP DAAC), USGS/Earth Resources Observation and Science (EROS) Center, Sioux Falls, South Dakota ([https://lpdaac.usgs.gov/get\\_data](https://lpdaac.usgs.gov/get_data)).

## Appendix A. Supplementary data

Supplementary data related to this article can be found at <http://dx.doi.org/10.1016/j.apgeog.2013.09.024>.

## References

- Adame, M. F., Kauffman, J. B., Medina, I., Gamboa, J. N., Torres, O., Caamal, J. P., et al. (2013). Carbon stocks of tropical coastal wetlands within the karstic landscape of the Mexican Caribbean. *PLoS One*, 8, e56569.
- Aksornkoae, S. (1993). *Ecology and management of mangroves*. Bangkok, Thailand: The IUCN Wetland Programme.
- Alongi, D. M. (2002). Present state and future of the world's mangrove forests. *Environmental Conservation*, 29(3), 331–349.
- Alongi, D. M. (2011). Carbon payments for mangrove conservation: ecosystem constraints and uncertainties of sequestration potential. *Environmental Science and Policy*, 14(4), 462–470.
- Alongi, D. M., & Dixon, P. (2000). Mangrove primary production and above and below-ground biomass in Sawi Bay, southern Thailand. *Phuket Marine Biological Center Special Publication*, 22, 31–38.
- Autodesk, Inc.. (2013). *Autodesk 123D*. Retrieved 01.05.13, from <http://www.123dapp.com>.
- Barbier, E. B. (2006). Natural barrier to natural disasters: replanting mangroves after the tsunami. *Frontiers in Ecology and the Environment*, 4, 124–131.
- Barbier, E. B., & Cox, M. (2004). Introduction: global mangrove loss and economic development. In E. B. Barbier, & S. Sathirathai (Eds.), *Shrimp farming and mangrove loss in Thailand*. UK: Edward Elgar Publishing Ltd.
- Breiman, L. (2001). Statistical modeling: the two cultures. *Statistical Science*, 16, 199–231.
- Chansang, H. (1984). Structure of a mangrove forest at Ko Yao Yai, southern Thailand. In E. Soepadmo, A. N. Rao, & D. J. MacIntosh (Eds.), *Proceedings of the Asian symposium on mangrove environment: Research and management* (pp. 86–105). Kuala Lumpur, Malaysia.
- Chen, Y., Li, X., Liu, X., & Ai, B. (2013). Analyzing land-cover change and corresponding impacts on carbon budget in a fast developing sub-tropical region by integrating MODIS and Landsat TM/ETM+ images. *Applied Geography*, 45, 10–21.
- Christensen, B. (1978). Biomass and productivity of *Rhizophora apiculata* Bl in a mangrove southern Thailand. *Aquatic Botany*, 4, 43–52.
- Cintron, G. M., & Schaeffer-Noeuvelli, Y. (1984). Methods for studying mangrove structure. In S. C. Snedaker, & J. G. Snedaker (Eds.), *Monographs on oceanographic methodology: Vol. 8. The mangrove ecosystem: Research methods* (pp. 91–113).
- Clough, B. F. (1992). Primary productivity and growth of mangrove forests. In D. M. Alongi, & A. I. Robertson (Eds.), *Tropical mangrove ecosystems, coastal and estuarine studies*. 41. Washington, D.C.: American Geophysical Union.
- Clough, B. F., & Scott, K. (1989). Allometric relationships for estimating above-ground biomass in six mangrove species. *Forest Ecology and Management*, 27, 117–127.
- CORIN (Coastal Resources Institute). (1995). *The effect of aquaculture on agricultural land and coastal environment*. Songkhla, Thailand: Prince of Songkhla University.
- Curtis, J. T., & McIntosh, R. P. (1950). The interrelations of certain analytic and synthetic phytosociological characters. *Ecology*, 31(3), 434–455.
- Donato, D. C., Kauffman, J. B., Mackenzie, R. A., Ainsworth, A., & Pfleeger, A. Z. (2012). Whole-island carbon stocks in the tropical Pacific: implications for mangrove conservation and upland restoration. *Journal of Environmental Management*, 97, 89–96.
- Donato, D. C., Kauffman, J. B., Murdiyarto, D., Kurnianto, S., Stidham, M., & Kanninen, M. (2011). Mangroves among the most carbon-rich forests in the tropics. *Nature Geoscience*, 4, 293–297.
- Doydee, P., & Buot, I. E., Jr. (2010). Mangrove habitat restoration and management in Ranong Province, Thailand. In *Proceeding of coastal zone Asia-Pacific conference and world small-scale fisheries congress*. Bangkok, Thailand.
- Duke, N. C., Meynecke, J.-O., Dittmann, S., Ellison, A. M., Anger, K., Berger, U., et al. (2007). A world without mangroves? *Science*, 317, 41–42.
- EEPSEA (Economy and Environment Program for Southeast Asia). (1998). *Economic valuation of mangroves and the roles of local communities in the conservation of natural resources: Case study of Surat Thani, South of Thailand*. Singapore: S. Sathirathai.
- Efron, B., & Gong, G. (1983). A leisurely look at the bootstrap, the jackknife, and cross-validation. *The American Statistician*, 37, 36–48.
- Fatoyinbo, T. E., Simard, M., Washington-Allen, R. A., & Shugart, H. H. (2008). Landscape-scale extent, height, biomass, and carbon estimation of Mozambique's mangrove forests with Landsat ETM+ and Shuttle Radar Topography Mission elevation data. *Journal of Geophysical Research*, 113, G02S06.
- Friess, D. A., Krauss, K. W., Horstman, E. M., Balke, T., Bouma, T. J., Galli, D., et al. (2012). Are all intertidal wetlands naturally created equal? Bottlenecks, thresholds and knowledge gaps to mangrove and saltmarsh ecosystems. *Biological Reviews*, 87, 346–366.
- Fujioka, Y., Tabuchi, R., Hirata, Y., Yonededa, R., Patanaponpaiboon, P., Poungparn, S., et al. (2008). Disturbance and recovery of mangrove forests and macrobenthic communities in Andaman Sea, Thailand following the Indian Ocean Tsunami. In *Proceedings of the 11th international coral reef symposium*. Ft. Lauderdale, Florida.
- Giri, C., Zhu, Z., Tieszen, L. L., Singh, A., Gillette, S., & Kelmelis, J. A. (2008). Mangrove forest distributions and dynamics (1975–2005) of the tsunami-affected region of Asia. *Journal of Biogeography*, 35, 519–528.
- GRASS Development Team. (2012). *Geographic resources analysis support system (GRASS) software*. Version 6.4.2. Open Source Geospatial Foundation. Retrieved 19.12.12 from <http://grass.osgeo.org>.

- Hall, M., Frank, E., Holmes, G., Pfahringer, B., Reutemann, P., & Witten, I. H. (2009). The WEKA data mining software: an update. *SIGKDD Explorations*, 11(1), 10–18.
- Heumann, B. W. (2011). Satellite remote sensing of mangrove forests: recent advances and future opportunities. *Progress in Physical Geography*, 35, 87–108.
- Huang, X., Zhang, L. P., & Wang, L. (2009). Evaluation of morphological texture features for mangrove forest mapping and species discrimination using multispectral IKONOS imagery. *IEEE Letters, Geoscience and Remote Sensing Letters*, 6, 393–397.
- Jordan, C. F. (1969). Derivation of leaf area index from quality measurements of light on the forest floor. *Ecology*, 50, 663–666.
- Kauffman, J. B., Heider, C., Cole, T. G., Dwire, K. A., & Donato, D. C. (2011). Ecosystem carbon stocks of Micronesian mangrove forests. *Wetlands*, 31, 343–352.
- Ketterings, Q. M., Coe, R., Noordwijk, M., Ambagau, Y., & Palm, C. A. (2001). Reducing uncertainty in the use of allometric biomass equations for predicting above-ground tree biomass in mixed secondary forests. *Forest Ecology and Management*, 146, 199–209.
- Klein, I., Gessner, U., & Kuenzer, C. (2012). Regional land cover mapping and change detection in Central Asia using MODIS time-series. *Applied Geography*, 35, 219–234.
- Komiyama, A., Havanond, S., Srisawatt, W., Mochida, Y., Fujimoto, K., Ohnishi, T., et al. (2000). Top/root biomass ratio of a secondary mangrove (*Ceriops tagal* (Perr.) C. B. Rob.) forest. *Forest Ecology and Management*, 139, 127–134.
- Komiyama, A., Ogino, K., Aksornkoae, S., & Sabhasri, S. (1987). Root biomass of a mangrove forest in southern Thailand. 1. Estimation by the trench method and the zonal structure of root biomass. *Journal of Tropical Ecology*, 3, 97–108.
- Komiyama, A., Ong, J. E., & Pongparn, S. (2008). Allometry, biomass, and productivity of mangrove forests: a review. *Aquatic Botany*, 89, 128–137.
- Komiyama, A., Pongparn, S., & Kato, S. (2005). Common allometric equations for estimating the tree weight of mangroves. *Journal of Tropical Ecology*, 21, 471–477.
- Kongsangcha, J., Patanaponpiboon, P., Komiyama, A., Higo, M., Havanond, S., Havanond, S., et al. (1993). *Rehabilitation programs of mangrove forest in Thailand*. Pro Natura Fund. The Nature Conservation Society of Japan. Retrieved 12.10.12, from <http://www.nacsj.or.jp/pn/houkoku/h01-08/h04-no17.html>.
- Lacambra, C., Friess, D., Spencer, T., & Moller, I. (2013). Bioshields: mangrove ecosystems as resilient natural coastal defences. In F. Renaud, K. Sudmeier-Rieux, & M. Estrella (Eds.), *The role of ecosystems in disaster risk reduction: From science to practice*. Tokyo: UNU Press.
- Macintosh, D. J., Aston, E. C., & Havanon, S. (2002). Mangrove rehabilitation and intertidal biodiversity: a study in the Ranong mangrove ecosystem, Thailand. *Estuarine, Coastal and Shelf Science*, 55, 331–345.
- Macintosh, D. J., Ashton, E. C., & Tansakul, V. (2002). *Utilisation and knowledge of biodiversity in the Ranong Biosphere Reserve, Thailand*. ITCZM monograph no. 7 (pp. 30).
- Mitra, A., Sengupta, K., & Banerjee, K. (2011). Standing biomass and carbon storage of above-ground structures in dominant mangrove trees in the Sundarbans. *Forest Ecology and Management*, 261, 1325–1335.
- Muda, A., & Mustafa, N. M. S. N. (2003). *A working plan for the Matang mangrove forest reserve, Perak* (Fifth revision). Malaysia: State Forestry Department of Perak Darul Ridzuan.
- My3DScanner, My3DScanner: *Replicate the world in 3D*. Retrieved 01.05.13, from <http://www.my3dscanner.com>.
- NASA Land Processes Distributed Active Archive Center (LP DAAC). (2012). *ASTER GDEM V2*. Sioux Falls, South Dakota: USGS/Earth Resources Observation and Science (EROS) Center.
- Ni, W., Guo, Z., Sun, G., & Chi, H. (2010). Investigation of forest height retrieval using SRTM-DEM and ASTER-GDEM. In *Geoscience and remote sensing symposium (IGARSS), 2010 IEEE international* (pp. 2111–2114).
- Paruelo, J. M., Jobbagy, E. G., Sala, O. E., Lauenroth, W. K., & Burk, I. (1998). Functional and structural convergence of temperate grassland and shrubland ecosystems. *Ecological Applications*, 8, 194–206.
- Pedregosa, F., Varoquaux, G., Gramfort, A., Michel, V., Thirion, B., Grisel, O., et al. (2011). Scikit-learn: machine learning in Python. *Journal of Machine Learning Research*, 12, 2825–2830.
- Phongsuksawat, P. (2002). *Determination of tree biomass in the mangrove habitat study area, Changwat Phangna* (Master's thesis). Thailand: Kasetsart University.
- Pineiro, G., Perelman, S., Guerschman, J. P., & Paruelo, J. M. (2008). How to evaluate models: observed vs. predicted or predicted vs. observed? *Ecological Modelling*, 216, 316–322.
- Pongparn, S. (2003). *Common allometric relationships for estimating the biomass of mangrove forests* (Doctoral dissertation). Japan: Gifu University.
- Putz, F. E., & Chan, H. T. (1986). Tree growth, dynamics, and productivity in a mature mangrove forest in Malaysia. *Forest Ecology and Management*, 17, 211–230.
- R Core Team. (2013). *R: A language and environment for statistical computing*. Vienna, Austria: R Foundation for Statistical Computing. Retrieved 01.05.13, from <http://www.R-project.org>.
- Rouse, J. W., Haas, R. H., Schell, J. A., & Deering, D. W. (1973). Monitoring vegetation systems in the great plains with ERTS. In *Third ERTS symposium, NASA SP-351 I* (pp. 309–317).
- Saenger, P. (2002). *Mangrove ecology, silviculture and conservation*. The Netherlands: Kluwer Academic Press.
- Schlerf, M., Atzberger, C., & Hill, J. (2005). Remote sensing of forest biophysical variables using HyMap imaging spectrometer data. *Remote Sensing of Environment*, 95, 177–194.
- Shevade, S. K., Keerthi, S. S., Bhattacharyya, C., & Murthy, K. R. K. (1999). Improvements to the SMO algorithm for SVM regression. *IEEE Transactions on Neural Networks*, 11, 1188–1193.
- Simard, M., Fatoyinbo, T. E., & Pinto, N. (2009). Mangrove canopy 3D structure and ecosystem productivity using active remote sensing. In Y. Wang (Ed.), *Remote sensing of coastal environments*. London: Taylor and Francis Group LLC.
- Simard, M., Zhang, K., Rivera-Monroy, V. H., Ross, M. S., Ruiz, P. L., Castaneda-Moya, E., et al. (2006). Mapping height and biomass of mangrove forests in Everglades National Park with SRTM elevation data. *Photogrammetric Engineering & Remote Sensing*, 72(3), 299–311.
- Smola, A. J., & Schoelkopf, B. (2004). A tutorial on support vector regression. *Statistics and Computing*, 14, 199–222.
- Soares, M. L. G., & Schaeffer-Novelli, Y. (2005). Above-ground biomass of mangrove species. Analysis of models. *Estuarine, Coastal and Shelf Science*, 65, 1–18.
- Spalding, M., Blasco, F., & Field, C. (1997). *World mangrove atlas*. Paris: International Society for Mangrove Ecosystems, World Conservation Monitoring Centre, National Council for Scientific Research.
- Sudtongkong, C., & Webb, E. L. (2008). Outcomes of state- vs. community-based mangrove management in southern Thailand. *Ecology and Society*, 13(2), 27. Retrieved 01.05.13, from <http://www.ecologyandsociety.org/vol13/iss2/art27/>.
- Tamai, S., & Iampa, P. (1988). Establishment and growth of mangrove seedlings in mangrove forest in southern Thailand. *Ecological Research*, 3, 227–238.
- Tamai, S., Nakasuga, T., Tabuchi, R., & Ogina, K. (1986). Standing biomass of mangrove forest in southern Thailand. *Journal of the Japanese Forestry Society*, 68(9), 384–388.
- Twilley, R. R., Chen, R. H., & Hargis, T. (1992). Carbon sinks in mangroves and their implications to carbon budget of tropical coastal ecosystems. *Water, Air, and Soil Pollution*, 64, 265–288.
- Valiela, I., Bowen, J. L., & York, J. K. (2001). Mangrove Forests: one of the world's threatened major tropical environments. *BioScience*, 51(10), 807–815.
- Wang, L., Silvan-Cardenas, J. L., & Sousa, W. P. (2008). Neural network classification of mangrove species form multi-seasonal IKONOS imagery. *Photogrammetric Engineering and Remote Sensing*, 74, 921–927.
- Wicaksono, P., Danoedoro, P., Hartono, H., Nehren, U., & Ribbe, L. (2011). Preliminary work of mangrove ecosystem carbon stock mapping in small island using remote sensing: above and below ground carbon stock mapping on medium resolution satellite image. In *Proceedings of SPIE: Vol. 8174. Remote sensing for agriculture, ecosystems, and hydrology XIII*.
- World Bank. (2011). *Mitigating climate change through restoration and management of coastal wetlands and near-shore marine ecosystems: Challenges and opportunities*. Environment Department paper 12. Washington, DC: Crooks, S., Herr, D., Tamelander, J., Laffolet, D., & Vandever, J.
- Yuen, J. Q., Ziegler, A. D., Webb, E. L., & Ryan, C. (2013). Uncertainty in below-ground carbon biomass for major land covers in Southeast Asia. *Forest Ecology and Management*.
- Ziegler, A. D., Phelps, J., Yuen, J. Q., Lawrence, D., Webb, E. L., Bruun, T. B., et al. (2012). Carbon outcomes of major land-cover transitions in SE Asia: great uncertainties and REDD+ policy implications. *Global Change Biology*, 18, 3087–3099.